Exceptional preservation of fossil plant spores in high-pressure metamorphic rocks

Sylvain Bernard [a,*], Karim Benzerara [b], Olivier Beyssac [a], Nicolas Menguy [b],
Francois Guyot [b], Gordon E. Brown Jr. [c], Bruno Goffé [a]

[a] *Laboratoire de Géologie, ENS-CNRS, 24 rue Lhomond, 75005 Paris, France*
[b] *IMPMC, CNRS UMR 7590, Dept. de Minéralogie IPGP, Université Paris 6 and 7, 140 rue de Lourmel, 75015 Paris, France*
[c] *Surface & Aqueous Geochemistry Group, Department of Geological and Environmental Sciences, Stanford University, Stanford, CA 94305-2115, USA*

Abstract

It is commonly believed that high-grade metamorphism erases all traces of fossils and, more generally, of biogenicity in rocks. To address this issue, we report in this study X-ray spectromicroscopy, Raman microspectroscopy, and electron microscopy observations at the nm-scale of fossil lycophytes megaspores found in Triassic metasedimentary rocks from the French Alps. These rocks have undergone high-pressure metamorphic conditions (~ 14 kbar, ~ 360 °C) during the Alpine orogeny corresponding to a burial of ~ 35 km during subduction. Despite such metamorphism, the fossil megaspores are remarkably well-preserved texturally. An unusual mineralogical zonation consisting of magnetite, ankerite and calcite is superposed on the structures of the spore walls. In parallel, chemical heterogeneities of the organic matter (OM) composing the spore walls were detected. We discuss different interpretations for our observations, in particular a scenario in which these features are remnants of the original structural heterogeneities in the spores, and provide insights on the fossilization processes under high-grade metamorphic conditions. Whatever the processes leading to such heterogeneities, our observations oppose the usual assumption that high-grade metamorphism erases all indications of biogenicity in rocks and open new avenues for investigation at the nm-scale of the evolution of organic matter during diagenesis and metamorphism.
© 2007 Elsevier B.V. All rights reserved.

1. Introduction

Carbonaceous material (CM) is pervasive in metasedimentary rocks and results mostly from the transformation of biogenic organic matter (OM) during diagenetic and metamorphic processes. In most geological settings, high-grade metamorphism is thought to erase traces of the original chemistry and structure of biological materials, preventing reconstitution of their geochemical heritage, either biogenic or abiotic (Moorbath, 2005). Such loss is a major limitation on the search for life in the geological record, especially with regards to the primitive Earth (Schopf et al., 2002; Brasier et al., 2002), as most of the rocks from this period have been metamorphosed. It may

---

* Corresponding author. Tel.: +33 1 44 32 22 77; fax: +33 1 44 32 22 00.
E-mail address: Sylvain.Bernard@ens.fr (S. Bernard).

also be an issue for the preservation of the fossil record in more recent periods. For instance, several Cambrian "konservat-lagerstätten" actually exhibit exceptionally well preserved soft-bodied organisms, and provide critical information on the origin of modern phyla and the evolutionary processes associated with the explosive diversification of life. Various studies have been dedicated to the preservation of OM in Cambrian fossils (Butterfield, 2003; Gaines et al., 2005; Zhu et al., 2005). These fossils have in general been submitted to various diagenetic processes (Knoll and Walter, 1992; Briggs, 2003), and more rarely to metamorphism as in the case of the Burgess Shale fossils, which underwent greenschist facies metamorphism (Butterfield, 1995; Orr et al., 1998; Powell, 2003; Butterfield et al., 2007). Whether some processes preserve those fossils from degradation during metamorphism is an important question to address. In a different perspective, a considerable research effort has now established the bulk chemical and structural evolution of coals and kerogens associated with hydrocarbon release during diagenesis and very low-grade metamorphism (Cody et al., 1996; Hemsley et al., 1996; Derenne and Largeau, 2001).

Under higher metamorphic conditions, the structural mechanisms of graphitization are well described (Buseck and Huang, 1985; Beyssac et al., 2002a) as they may be used as indicators of metamorphic grade (Wopenka and Pasteris, 1993; Beyssac et al., 2002b), but the chemical transformations involved in graphitization as well as the relationships between OM and minerals remain largely unknown. Some fossils have been described in high-grade metamorphic rocks, but these observations are mostly restricted to morphological descriptions (Franz et al., 1991), and rarely focus on the structure and/or chemistry of the OM or minerals constituting the fossil itself (Goffé and Villey, 1984). Organic fossils have classically been studied using harsh chemical digestion procedures to extract the organic fraction from the sample. However, the recent development of *in situ* analytical techniques and sample preparation methods provides new opportunities for the study of such complex objects (Kempe et al., 2005) and for reducing occurrences of experimental contamination. In particular, we can get a better understanding of the origin of metamorphic OM preserved in fossils and associated minerals as well as of the mechanisms of their preservation by combining the structural and chemical characterization of these objects from the millimeter- down to the nanometer-scale.

In this study, we have selected fossilized objects which have experienced a metamorphic cycle involving high-pressure, low-temperature (HP–LT) conditions in the blueschist facies, and a complex but well-known tectonic history. Identification of the biological structures in these objects is not limited to the morphology of the fossils, but also includes submicrometer-scale chemical and structural features. These observations were made possible by a novel combination of microstructural and microchemical analytical techniques including Raman microspectroscopy (RM), scanning transmission X-ray microscopy (STXM), and transmission electron microscopy (TEM). Use of these methods does not require that the fossils be removed from the enclosing rock. By comparing our observations with the structure and chemistry of modern spores, we discuss the eventual preservation of biostructural features following high-grade metamorphism.

2. Geological setting and sample description

2.1. Geological setting

Samples were collected in Triassic CM-rich (3 wt. %) (Goffé and Villey, 1984) limestones at the Roc de la Pêche-Chanrossa in the Vanoise massif, Western Alps (France). The sampled formation was deposited in bauxitic karsts in a lacustrine environment during the Lettenkohle (ca. 225 Ma) (Ellenberger, 1958), and was involved in the Alpine orogenesis, with a deep burial during subduction followed by exhumation within the orogenic wedge. The mineral assemblage of the Roc de la Pêche-Chanrossa includes Mg–carpholite, chloritoid, lawsonite, aragonite, and phengite. It indicates HP–LT metamorphic conditions in the blueschist facies. Fig. 1 depicts a P–T diagram with the index mineralogy encountered in these rocks; isopleths have been calculated for the chemical compositions of minerals analyzed in these rocks. The presence of aragonite, Mg–carpholite and lawsonite within these rocks puts a lower bound for the peak of pressure, while the maximum Si content of phengites is a quantitative proxy to estimate the peak pressure at ∼14 kbar (Massonne and Szpurka, 1997). Peak temperature is constrained by the Fe–Mg exchange between Mg–carpholite and chloritoid at ∼360 °C, in excellent agreement with the temperature estimated from Raman spectroscopy of CM thermometry at ∼360 °C (see below). These metasediments followed a counter-clockwise metamorphic cycle (Gillet and Goffe, 1988) (Fig. 1), with peak conditions at ∼14 kbar and 360 °C, corresponding to a burial depth of nearly 35 km during subduction. Fast exhumation of these rocks in less than 15 Myr along a cold gradient of 10 °C/km has been proposed, in order
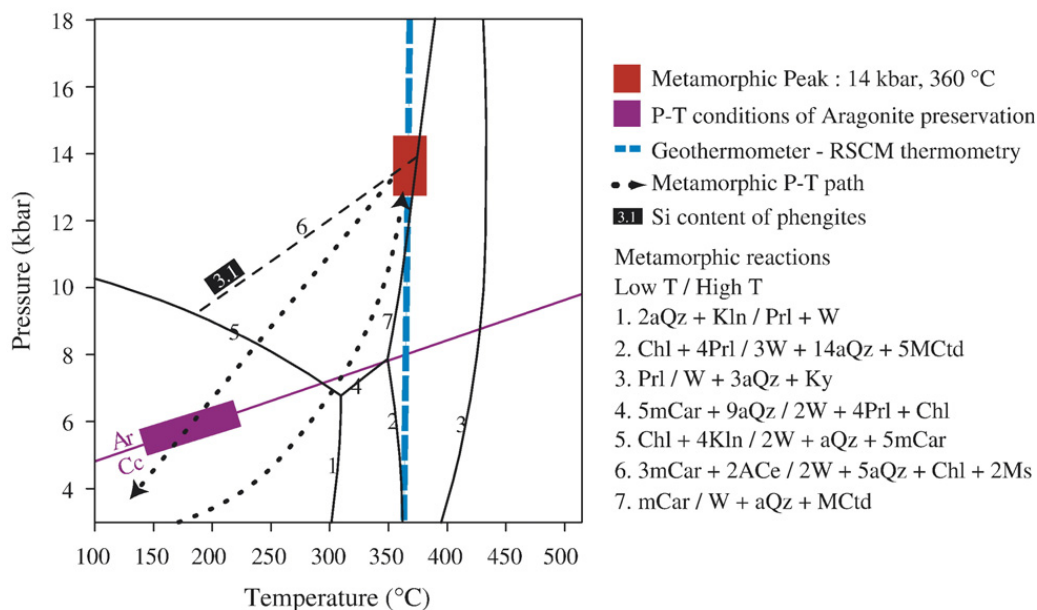
Fig. 1. Pressure–temperature diagram summarizing the metamorphic conditions for the Vanoise massif (Western Alps, France). The position of all the isopleth curves was specifically calculated for the mineral compositions analyzed in the Vanoise samples. The tentative *P–T* path is modified from Gillet and Goffe (1988) who discussed the *P–T* conditions necessary for aragonite preservation. RSCM is Raman Spectroscopy of Carbonaceous Material (Beyssac et al., 2002b). Mineralogical abbreviations after Kretz (1983).

to account for the preservation of the HP–LT mineral assemblage (Gillet and Goffe, 1988).

2.2. Sample description

The samples examined are carbonated septaria, which are concretions formed during shallow burial by lithification of soft sediments and which are believed to provide an efficient protection to soft tissue fossils during diagenetic processes (*e.g.* Cope and Curtis, 2000). Within the septaria, some metamorphic minerals, mostly phengites, are observed with chemical compositions similar to those analyzed in the host-rock matrix. Vegetal tissue debris are texturally well preserved in these septaria, particularly some sections of tracheid tissues and those of ∼ 300 μm diameter which were identified as late middle-Triassic lycophyte megaspores (Fig. 2). The identification of these debris as lycophyte megaspores was first made by Goffé and Villey (1984) based on ultrastructural criteria, then confirmed by two specialists of these fossils (Lea Grauvogel-Stamm, personal communication, 2005; and Bernard Lugardon, personal communication, 2005). The observation of other plant tissues such as conducting tissues also contributes to the identification of the biological origin of these debris. Moreover, lycophytes spores are widely used as stratigraphic fossils, and their ultrastructure is well known. The megaspore wall, as inferred from modern and fossil examples, has a characteristic structure with two well-defined layers

(Erdtman, 1969; Gabarayeva and Hemsley, 2006). The outer layer (exospore) is mostly composed of sporopollenin, a biopolymer highly resistant to mechanical and chemical degradation. This exospore, which generally exhibits ornamentations, might be preserved in diagenetic and/or metamorphic samples (Hemsley et al., 1996). The less resistant inner layer (endospore) is made of cellulose and pectates and is usually not preserved in fossil megaspores (Hemsley et al., 1996; Hanel et al., 1999). It is generally assumed that the ultrastructure of megaspore walls is correlated with their taxonomic position thus allowing their identification by microscopy observations (Wang and Wang, 1982; Morbelli, 1995; Cantrill and Webb, 1998; Lugardon et al., 2000; Cottnam et al., 2000; Grauvogel-Stamm and Lugardon, 2001; Macluf et al., 2003; Grauvogel-Stamm and Lugardon, 2004). For example, the size, the number of sublayers in the exospore, the ornamentation of the external layer, and the presence of apertures are used for such palynological identification. The Vanoise fossils are around 300 to 400 μm in diameter; they show specific ornamentations and concentric layering. They display numerous ultrastructural similarities with lycophyte megaspores in general (see, *e.g.*, Cottnam et al., 2000 plate I, Fig. 1, or Macluf et al., 2003 plate V), and more specifically with Triassic lycophyte spores found in the non-metamorphic Lettenkohle deposits from Alsace (France) (Grauvogel-Stamm and Duringer, 1983), which formed at the same period as the metamorphosed sediments from Vanoise.

3. Analytical methods

3.1. Raman microspectroscopy and compositional mapping

Raman data were obtained with a Renishaw INVIA spectrometer (ENS Paris). Spectra were measured at a constant temperature (~20–22 °C) with the 514.5 nm wavelength of a 20 mW spectra physics Argon laser focused through a Leica microscope with a 50× objective (NA=0.75). This configuration yields a planar resolution <2 μm and a laser power delivered at the sample surface of around 1 mW (an instrumental configuration which is well below the threshold value that results in radiation damage to the sample analyzed). Light was dispersed by a holographic grating with 1800 grooves/mm and the signal analyzed with a RENCAM CCD detector.

For Raman mapping, we used the spectrometer described above with an XYZ motorized stage and a line

Fig. 2. Reflected light photomicrographs showing well-preserved lycophyte megaspores in petrographic thin sections of Triassic septaria from the Vanoise massif. In the upper photomicrograph, the megaspore is filled with calcite, while in the lower one, it is filled with phengite.

focus system which allows multiple acquisitions during a single measurement. To obtain compositional maps, an area enclosing all or part of a megaspore section was defined; the sampling step size was around 1 μm; the backscattered spectra obtained in each selected area were collected using the system described above. Each spectrum was subsequently compared to reference mineral spectra using the algorithm calculation of the software Wire 2.0 provided by Renishaw.

3.2. Sample preparation by focused ion beam milling

Focused ion beam (FIB) milling was performed with a FEI Model 200 SEM FIB system at the University Aix-Marseille III. The FIB lift-out method was used to prepare two cross-sections across the cell wall of two different fossil spores from Vanoise (see Fig. 3) in order to check the reproducibility of the measurements. This method is described in detail in Heaney et al. (2001) and Benzerara et al. (2005a). First, the cell wall of a megaspore was easily located using the imaging capabilities of the FIB-SEM. A thin layer of platinum was then deposited on the specimen across the cell wall in order to protect it during the milling process. The FIB system uses a Ga liquid metal ion source for milling. A 30 kV Ga^+ beam operating at ~20 nA excavated the sample from both sides of the Pt layer to a depth of 5 μm. Before removal of the thin section, the sample was further thinned to ~80 nm with a glancing angle Ga^+ beam at much lower beam currents of ~100 pA. Finally, a line pattern was drawn with the ion beam along the side and bottom edges of the thin section allowing its removal. The ~15 μm × 5 μm × 80 nm section was transferred at room pressure with a micromanipulator onto the membrane of a carbon-coated 200 mesh copper grid for subsequent TEM and STXM analyses. The obtained foils, whose thickness is estimated to be 80 nm, thus making it electron and soft X-ray transparent, are shown on Fig. 4.

3.3. STXM and NEXAFS spectroscopy

Scanning transmission X-ray microscopy (STXM) was used to perform high spatial and energy resolution near-edge X-ray absorption fine structure (NEXAFS) spectroscopy at the C K-edge (in the energy range 280 to 310 eV) and the Fe $L_{2,3}$-edges (in the energy range 700 to 730 eV). STXM is a transmission microscopy using a monochromated X-ray beam produced by synchrotron radiation. Protocols for STXM data acquisition and analysis and examples of applications can be found in Hitchcock (2001), Jacobsen et al. (2000) and Bluhm et al. (2006). STXM has been increasingly applied to
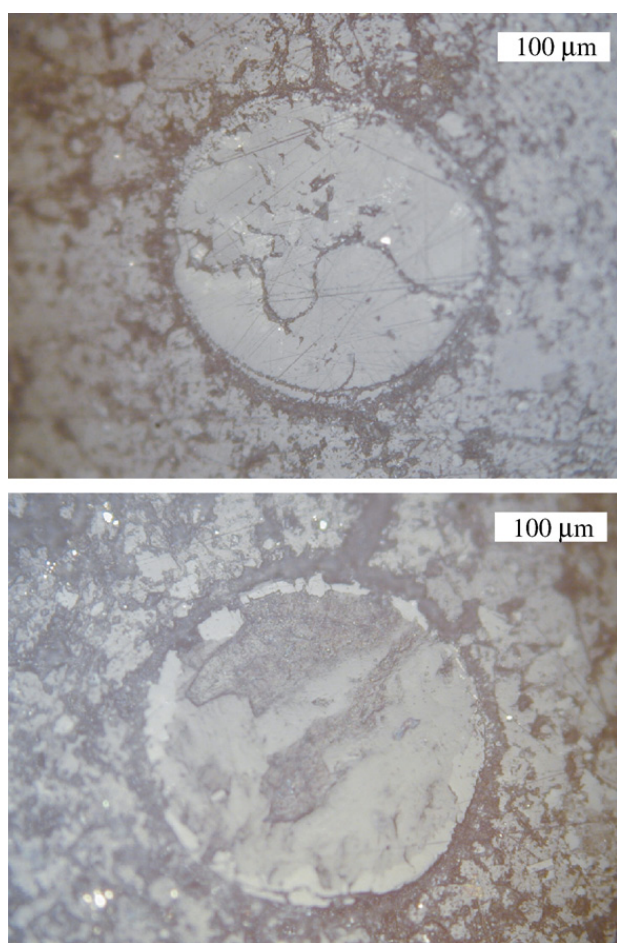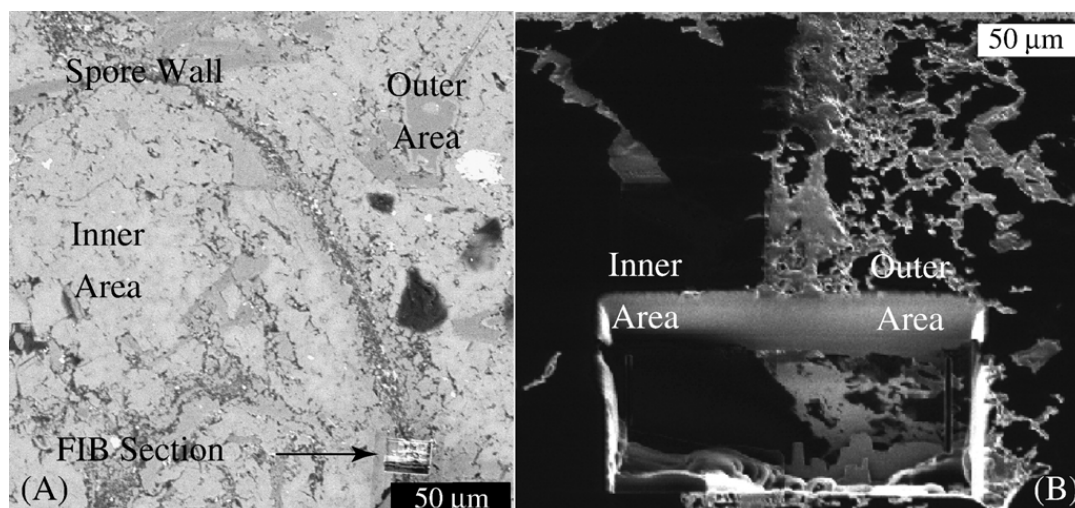
Fig. 3. Location of the FIB section 1. A. SEM photomicrograph of a lycophyte spore section showing the location of the FIB section 1. B. FIB image of the ultrathin section 1 before the micromanipulator-assisted extraction stage.

Earth science problems during the last 20 years (*e.g.*, Cody et al., 1998; Boyce et al., 2002; Jokic et al., 2003; Yoon et al., 2004; Schumacher et al., 2005; Benzerara et al., 2006a; Kinyangi et al., 2006; Dynes et al., 2006).

The energy of the X-ray beam on the ALS BL 11.0.2.2 STXM can be varied by less than 0.1 eV increments over a wide energy range (130–2100 eV). The beam is focused on the sample using a condenser zone plate and a 2-D image is collected by scanning the sample stage at a fixed photon energy. The image contrast results from differential absorption of X-rays, which depends on the chemical composition of the sample. C K-edge and Fe $L_{2,3}$-edge NEXAFS spectra can be collected by performing image stack acquisition or line scans. Image stacks or line scans were taken by scanning the sample in the x–y directions (image stack) or x direction (line scan) of selected sample areas at energy increments of 0.1 eV over the energy range of interest (280 to 310 eV for carbon, 700 to 730 eV for iron). Here, x refers to the horizontal direction, y to the vertical direction, and the x–y plane to the plane perpendicular to the X-ray beam direction. The stack image procedure thus consists of measuring the NEXAFS spectrum for a specific element on each pixel (one pixel can be as small as 30 nm) of the image. Counting times are of the order of few milliseconds or less per pixel. Normalization and background correction of the Fe $L_{2,3}$-edge and C K-edge NEXAFS spectra were performed by dividing each spectrum by a second spectrum from a Fe- or C-free location on the same sample. AXis2000 software (ver2.1n) (A.P. Hitchcock, 2000) was used to align image stacks and extract NEXAFS spectra from image stack or line scan measurements.

STXM measurements at the C K-edge were carried out on beamline 11.0.2.2 at the Advanced Light Source (Berkeley, USA) following the procedures described in Benzerara et al. (2004) and Bluhm et al. (2006). The synchrotron storage ring operated at 1.9 GeV and 200–400 mA stored current. A 1200 l/mm grating and 40 μm exit slit were used for imaging and spectroscopy, providing a theoretical energy resolution of 72 meV. Energy calibration was accomplished using the well-resolved 3p Rydberg peak at 294.96 eV of gaseous CO2 for the C K-edge. The different peaks observed in NEXAFS spectra on the spore wall measured at the C K-edge were tentatively indexed based on numerous previous NEXAFS studies on coal and natural carbon particles. A detailed discussion of NEXAFS spectroscopy can be found in Stohr (1992). Extensive databases of reference NEXAFS spectra measured on hundreds of compounds at the C K-edge, in some cases supported by theoretical calculations using multiple scattering approaches (*e.g.*, Stohr, 1992), are available (*e.g.*, http://unicorn.mcmaster.ca/corex/cedb-title.html; Ahuja et al., 1996; Myneni, 2002). STXM analyses at the Fe $L_{2,3}$-edges were carried out on beamline Pollux at the Swiss Light Source (SLS) at the Paul Scherrer Institut (Viligen, Switzerland). The SLS synchrotron storage ring was operated at 2.4 GeV and 190 mA current in a top-up mode during data collection.

3.4. TEM–EDSX

Transmission electron microscopy (TEM) studies were carried out on a Jeol 2100F microscope operating at 200 kV (IMPMC Paris), equipped with a field emission gun, a high-resolution UHR pole piece, and a
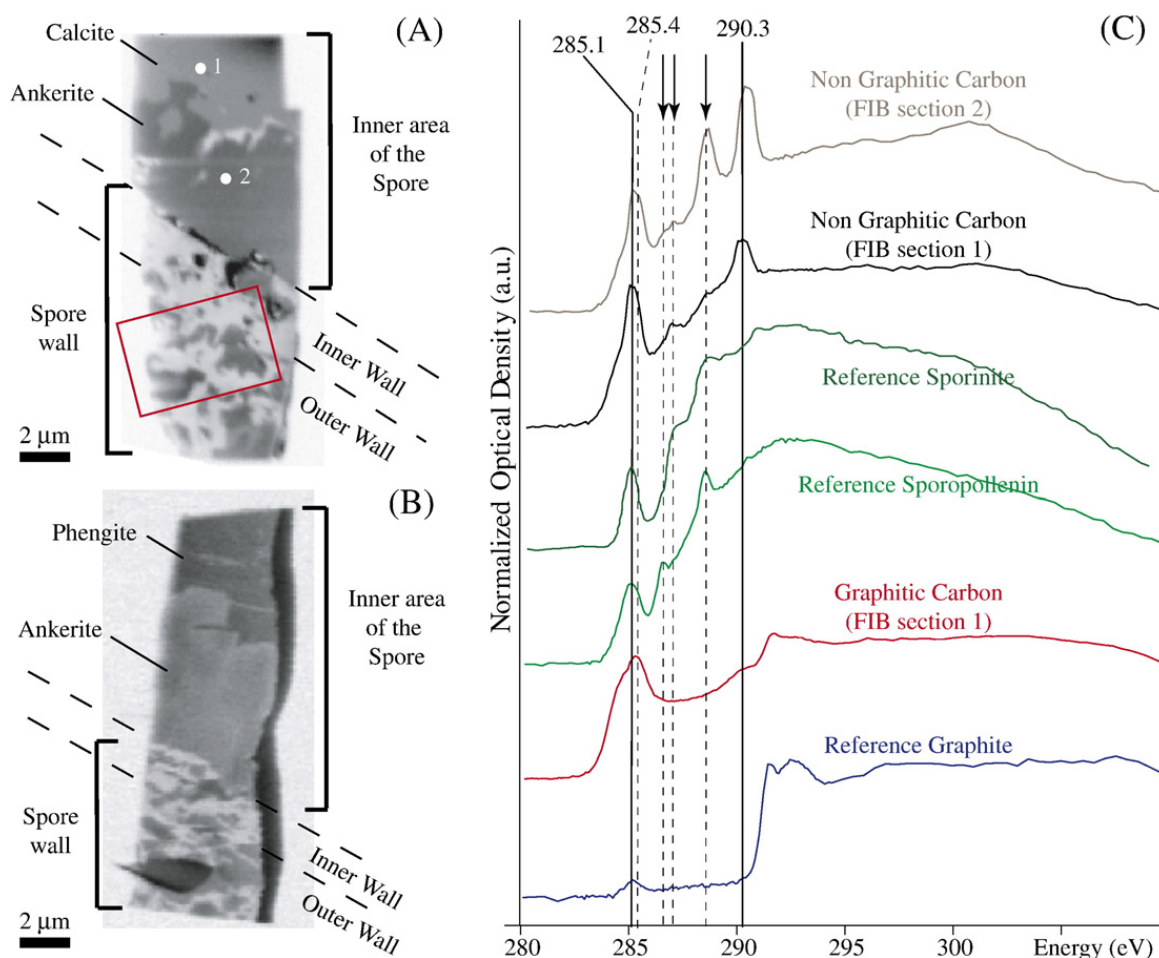
Fig. 4. STXM characterization of organic matter composing the spore walls. A. STXM image below the C K-edge at 280 eV (OM appears in bright spots) of the first FIB section showing ankerite and calcite. The red box indicates the position of the TEM photomicrograph shown in Fig. 6. The white spots (1 and 2) indicate the location of the EDXS analyses shown in Fig. 7. B. STXM at 280 eV (OM appears in bright spots) of the second FIB section showing ankerite and phengite. C. NEXAFS spectra of the different types of carbon observed in the FIB sections: Non-Graphitic Carbon (black spectrum for the FIB section 1, brown spectrum for the FIB section 2) and Graphitic Carbon (Red spectrum). Reference spectra of sporopollenin (green spectrum), sporinite (Cody et al., 1996) (dark green spectrum) and of graphite (blue spectrum) are shown for comparison. The relative amplitudes of the 285 and the 292 eV peaks of the graphite spectrum can simply vary due to the crystallographic orientation of the crystal (polarization effects) without reflecting any variation of chemistry (Atamny et al., 1992). Arrows at 286.7, 287.2, and 288.7 eV highlight peaks assigned, respectively, to ketone, phenol, and carboxylic groups. (For interpretation of the references to colour in this figure legend, the reader is referred to the web version of this article.)

Gatan energy filter GIF 200. Energy dispersive X-ray spectrometry (EDXS) analyses were performed using a JEOL detector with an ultrathin window allowing detection of light elements.

4. Results

4.1. Submicrometer-scale characterization of OM composing spore walls

Optical microscopy and RM investigations show that CM is widespread in the septaria, either in the spore walls or disseminated among minerals. Raman spectra of OM composing the megaspore walls are identical in terms of peak position, relative peak width, and relative height to spectra from OM debris dispersed in the matrix. All of these spectra systematically show two dominant features: vibrational bands at 1350 cm^{-1} (D1 defect band) and a broad band at ~ 1600 cm^{-1} (including graphite G band and D2 defect band), which are characteristic of graphitic but disordered CM (Beyssac et al., 2003) (Fig. 5). As RM reflects quantitatively the degree of structural organization of metamorphic CM, the structural organization of CM seems to be homogeneous throughout the sample examined. Raman spectroscopy was used to obtain geothermometry on CM (Beyssac et al., 2002b), and the peak metamorphic temperature was estimated to be ~ 360 °C, which is in agreement with that derived from
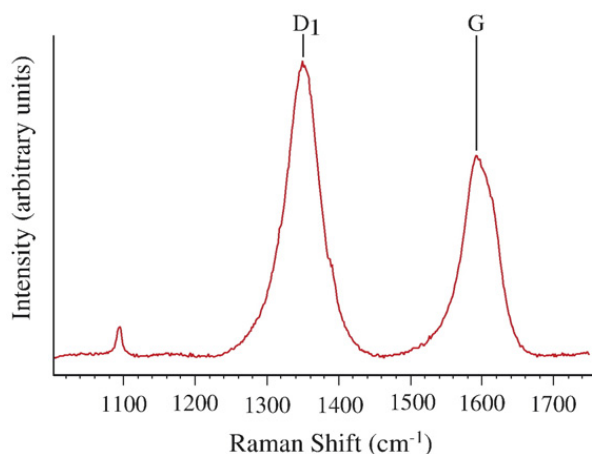
Fig. 5. Raman spectrum of organic matter found in Vanoise septaria. This spectrum shows two dominant features: vibrational bands at ∼1350 cm^{-1} (D1 — defect band) and ∼1600 cm^{-1} (includes G — graphite band and D2 — defect band), which are characteristic of graphitic but disordered CM (Beyssac et al., 2003). The estimation of temperature by the RSCM thermometry indicates that septaria from the Vanoise massif have reached a peak metamorphic temperature of ∼360 °C (Beyssac et al., 2002b).

conventional geothermometry based on the mineral assemblage.

At the submicrometer scale, STXM and TEM observations show two different concentric portions within the carbonaceous megaspore wall: an inner wall, around 3 µm thick, which is composed almost exclusively of OM, and an outer wall which is a mixture of OM and carbonates (Fig. 4). While the actual thickness of the entire outer wall varies from 10 µm to 50 µm in width, FIB sections contain only the first 4 to 5 µm of the outer wall in addition to the inner wall. NEXAFS spectra from both areas of the megaspore wall are significantly different indicating that they contain different C-bearing functional groups (Cody et al., 1996; Boyce et al., 2002). NEXAFS spectra from the outer wall indicate the presence of both aromatic carbon groups (285.1 eV interpreted as aromatic or olefinic C (1s–1π∗) and 292.8 eV indexed as C–C, aromatic (1s–σ∗); Cody et al., 1996) and saturated carbon as major constituents. The 286.7 eV peak indicates the presence of ketone (Cody et al., 1996). Phenolic groups (287.2 eV) are present only in small quantities. The 288.7 eV peak is indicative of carboxylic groups, which may be associated with fatty acids, whereas the 290.3 eV peak is characteristic of carbonate functional groups. In contrast, the NEXAFS spectrum of the inner carbon wall is more similar to that of graphite (Atamny et al., 1992) (Fig. 4). The differences in relative intensity of the peak at 285 eV between the spectrum obtained on the inner carbon wall and the reference spectrum of

graphite may result either from different crystallographic orientations (polarization effects) or more likely from different crystallinities of carbon (i.e. a poorly ordered carbon compound vs. a well-crystallized graphite); both effects may have a significant impact on the NEXAFS spectrum of the compound. As for the outer wall, the 290.3 eV peak of the inner-wall spectrum is characteristic of carbonate functional groups. The observation of two chemically different OM layers in the megaspore wall is further supported by TEM (Fig. 6), which shows two different microtextures in the outer and inner wall: a non-graphitic amorphous-like texture with vesicles of about 20 nm in diameter in the outer wall of the megaspore (Fig. 6B), and a denser graphitic texture (Fig. 6C) in the inner wall with a few 002 lattice fringes barely visible by HRTEM.

4.2. Detection and characterization of carbonates and iron oxide nanocrystals

Several remarkable mineralogical features were observed in association with the megaspore structure. First, two types of carbonates were detected by EDXS (Energy dispersive X-ray spectroscopy) in one of the FIB sections: pure calcite (CaCO$_3$) (Fig. 7A) and ankerite ((Mg,Fe)Ca (CO$_3$)$_2$) (Fig. 7B). Interestingly, the difference in compositions between calcite and ankerite induces a significant shift in the positions of the internal CO$_3$ stretching mode and the lattice modes in the Raman spectrum (Fig. 8). These differences can be used for discriminating calcite from ankerite. Fig. 8 presents a Raman map of a spore section within the septaria that shows the spatial distribution of ankerite and calcite. Ankerite is systematically observed as a ∼5 µm thick wavy layer beneath the carbonaceous megaspore walls. The rest of the megaspores are filled either with calcite or phyllosilicates such as phengite (Fig. 8). The septaria matrix is predominantly composed of pure calcite, with some sparse ankerite crystals systematically associated with organic debris. Consistently, ankerite was also detected in the second FIB section, comprising a layer beneath the spore wall, but most of the central part of the spore is occupied by phengite instead of calcite in this section (Fig. 4).

Furthermore, a 200 nm-thick layer of iron oxide nanocrystals (not detected by Raman) was observed adjacent to the inner, graphitic OM area on both FIB sections by TEM and STXM (Fig. 9). Electron diffraction patterns of these crystals are consistent with magnetite and/or maghemite, and indicate that the nanocrystals share a common crystallographic orientation parallel to the spore wall surface (Fig. 9). NEXAFS
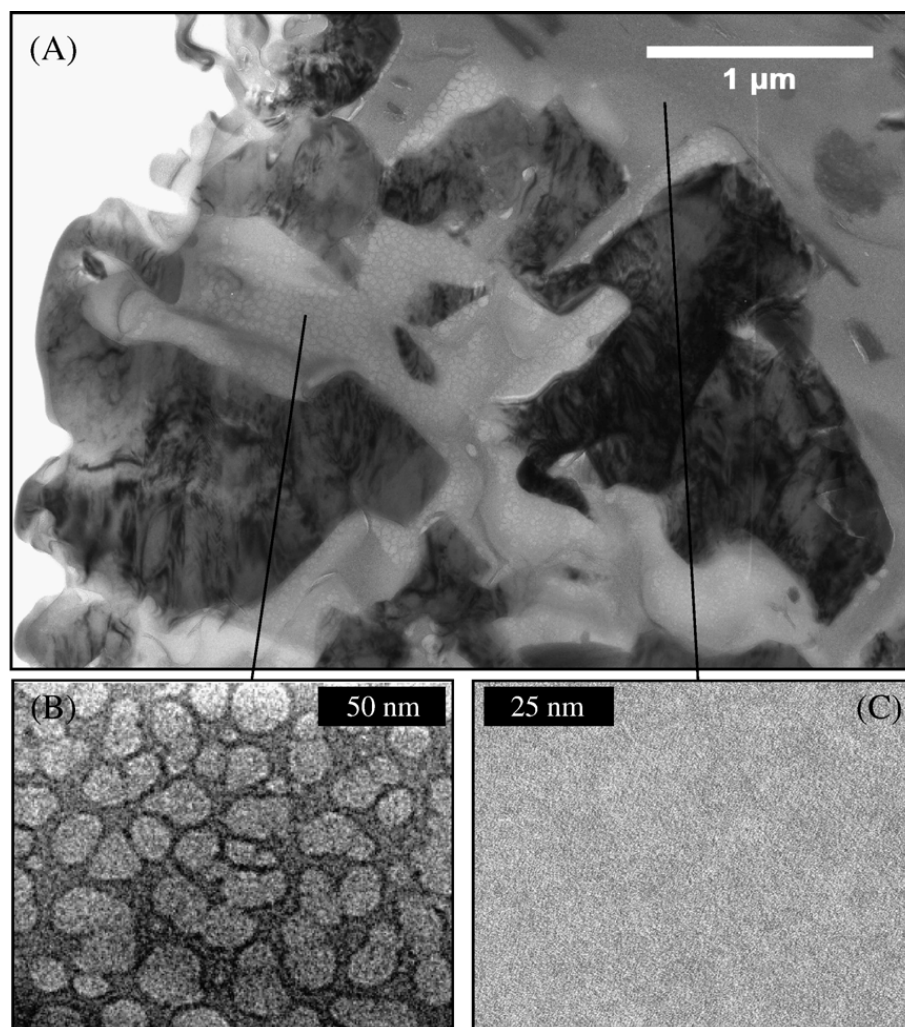
Fig. 6. TEM characterization of organic matter comprising the spore walls. A. TEM photomicrograph of organic matter comprising the spore wall located in Fig. 4A. B. TEM photomicrograph of non-graphitic organic matter. C. TEM photomicrograph of graphitic organic matter.

spectra at the Fe $L_{2,3}$ (2p1/2,3/2→3d) edges of these nanoparticles provide qualitative information on the $Fe^{3+}/\sum Fe$ ratio and hence help in discriminating between maghemite and magnetite (Peng et al., 1995; Brice-Profeta et al., 2005; Benzerara et al., 2005b). NEXAFS spectra measured on the iron oxide nanocrystals show two peaks at 707.8 and 709.4 eV, the latter being slightly stronger. Comparison with reference spectra of maghemite and magnetite suggests that the iron oxide nanocrystals in the spore wall are magnetites with some partial maghemitization (Fig. 9C).

5. Discussion

5.1. Potential contamination sources

Contamination is an important issue as illustrated for instance by the various debates on the finding of putative traces of life in meteorites (e.g., Jull et al., 1998; Benzerara et al., 2006b) or the identification of biomarkers in Archean samples (e.g., Dutkiewicz et al., 2006). Two sources of contamination are possible: one, experimental, during the handling and the preparation of the sample; the other, in the field, which would result in the contamination of the metamorphosed rocks after their exhumation, by natural OM. The latter would consequently not have undergone high-grade metamorphism in the blueschist facies. We first emphasize that the *in situ* analyses performed here, using microscopy techniques with no prior chemical extraction, allow characterization of OM that is intimately embedded within the minerals comprising the metamorphosed rocks, and so avoid carbon that would have been artefactually introduced during sample preparation. Moreover, RM analysis of OM has been performed within the thin section by focusing the laser on CM located beneath the surface of a transparent adjacent grain as previously suggested by Beyssac et al. (2003). Such CM situated within the section thickness was
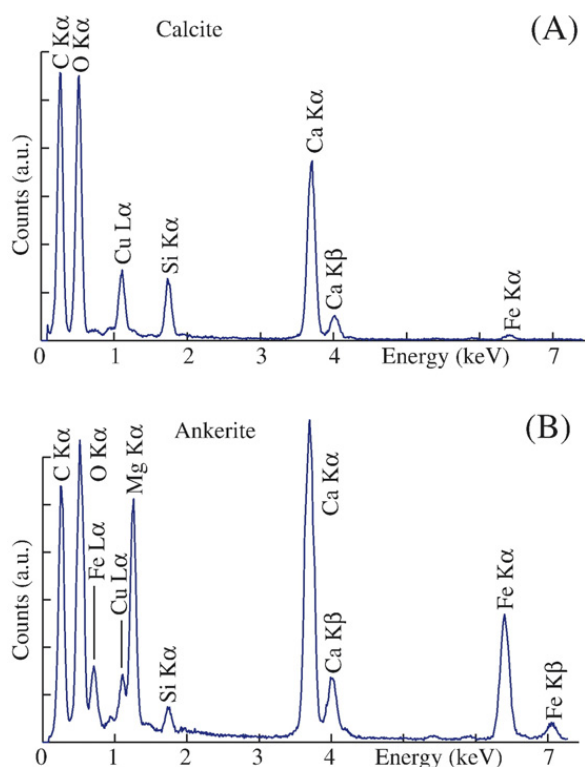
Fig. 7. EDXS analysis of carbonates associated with organic matter in the megaspores. A. EDXS analysis of a calcite crystal (CaCO$_3$) inside a spore (location shown by the white spot 1 in Fig. 4A). B. EDXS analysis of an ankerite crystal [(Fe,Mg)Ca(CO$_3$)$_2$] located at the contact with the same spore cell wall (location shown by the white spot 2 in Fig. 4A).

therefore not exposed at the surface of the thin section during polishing. In a similar way, FIB milling allowed us to prepare *in situ* an ultrathin section ensuring that the sampled volume is indeed part of the rock.

Finally, the possibility of an exogenous source for the megaspores can be definitely discounted as these megaspores have obviously undergone metamorphism. Indeed, RM measurements show that the degree of structural organization of OM within spore walls is consistent with metamorphic temperature of about 360 °C, which is the very same temperature as determined by conventional mineral geothermometry. This heating is confirmed at the nm-scale by NEXAFS spectroscopy at the C K-edge, which shows that some OM within the spore walls is slightly graphitized and has thus undergone metamorphism. Finally, phengites, which are undoubtedly metamorphic, have been observed within the megaspores, hence showing that the latter underwent metamorphism. Thus, the only carbon compound for which a late contamination origin in the field remains unchallenged is the ketone/phenol/carboxyl containing carbon (non-graphitic carbon). On one hand, the preservation of such functional groups under

HP–LT metamorphic conditions is surprising, as detailed below. On the other hand, we do not know any process that could insert large amounts of exogeneous carbon after exhumation of the likely poorly porous septarias. Moreover, the striking resemblance between the NEXAFS spectra of this carbon and sporopollenin suggests that this carbon is a metamorphic product of sporopollenin. A study of the evolution of the NEXAFS spectrum of sporopollenin at the C K-edge under high temperatures and pressures could help to determine if the preservation of the sporopollenin functional groups is expected and if protection by the septaria structures is necessary. While future studies on the origin of this carbon would be important, we will consider this carbon in the rest of the discussion as indigeneous.

5.2. Origin of the chemical, mineralogical, and textural heterogeneities within the megaspore wall

The OM-rich layer of the Vanoise megaspore wall shows chemical, mineralogical, and textural heterogeneities at the nanometer-scale. Heterogeneity affects OM comprising the cell wall: the outer part of the OM-rich layer is a mix of mostly non-graphitic OM and carbonate microveins, whereas the inner part is almost exclusively composed of partially graphitized OM. These chemical and textural heterogeneities may reflect the presence, or absence, of the carbonate microveins in a primarily homogeneous cell wall. In this case, carbonates would protect OM against chemical and structural changes during diagenesis and metamorphism. Another possibility is that these heterogeneities reflect original heterogeneities in the megaspores, and result from the differential preservation of the various biochemical structures present in non-metamorphosed megaspore cell walls. This alternative scenario is discussed further below.

A second type of heterogeneity is observed in the Vanoise megaspores in the form of an unusual mineralogical zonation consisting of distinct layers of magnetite, ankerite, and calcite or phyllosilicates. Different scenarios may be proposed to explain the formation of these mineralogical heterogeneities including the following: (1) Magnetite may derive from thermal degradation of an Fe-rich carbonate (such as siderite or Fe-rich ankerite) during metamorphism (Van Zuilen et al., 2003); however, it is difficult to reconcile such a process with the formation of two well-separated layers as well as the preferential crystallographic orientation of the magnetite crystals; in addition, one would expect to find a Mg- and Ca-rich, *i.e.* an Fe-
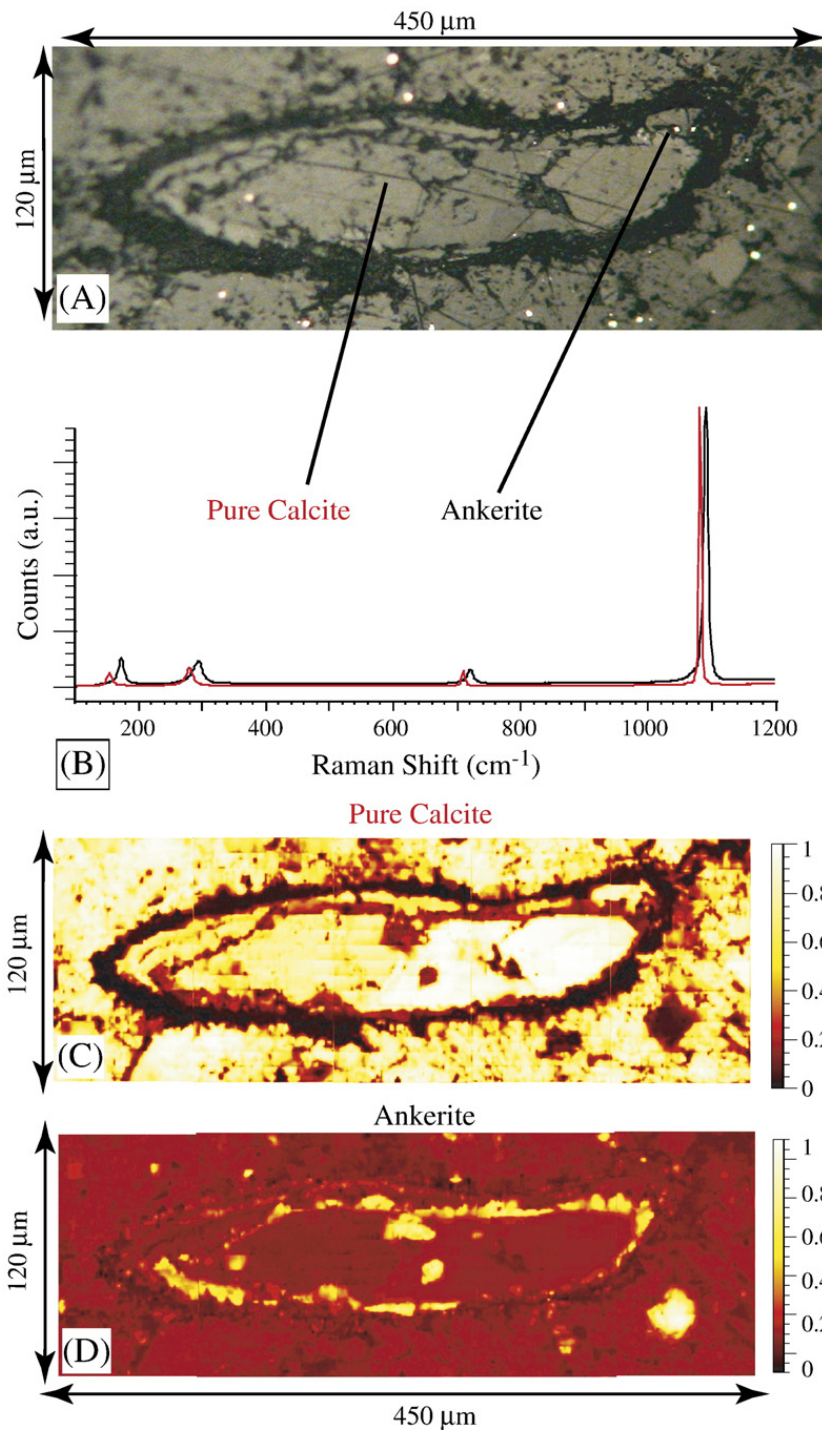
Fig. 8. Raman characterization of carbonates associated with a megaspore within the septaria. A. Optical photomicrograph showing a lycophyte megaspore from the same septaria in which the megaspores depicted in Fig. 2 were found. B. Raman spectra of the minerals present in the central part of the spore and beneath the spore cell wall, respectively, pure calcite (red spectrum: vibrational bands at 155, 280, 710 and 1085 cm^{-1}) and ankerite (black spectrum; this spectrum shows a shift to higher frequencies of about 15 cm^{-1} compared to the calcite reference spectrum). C. and D. Raman mapping showing the correlation index of each spectrum with the reference spectrum of pure calcite (C) and ankerite (D), respectively (mosaics compiled from ∼40,000 Raman spectra). Higher index values indicate a greater correlation between the sampled spot and the reference. Calcite thus appears as yellow/white in C. and ankerite appears as yellow/white in D.

depleted layer, which was not detected. (2) Another possibility is that precipitation of the magnetite and the ankerite layers did not occur simultaneously and that

some conditions (*e.g.*, pCO$_2$, oxygen fugacity, or temperature) may have changed between the two precipitation events favouring one mineralogy versus
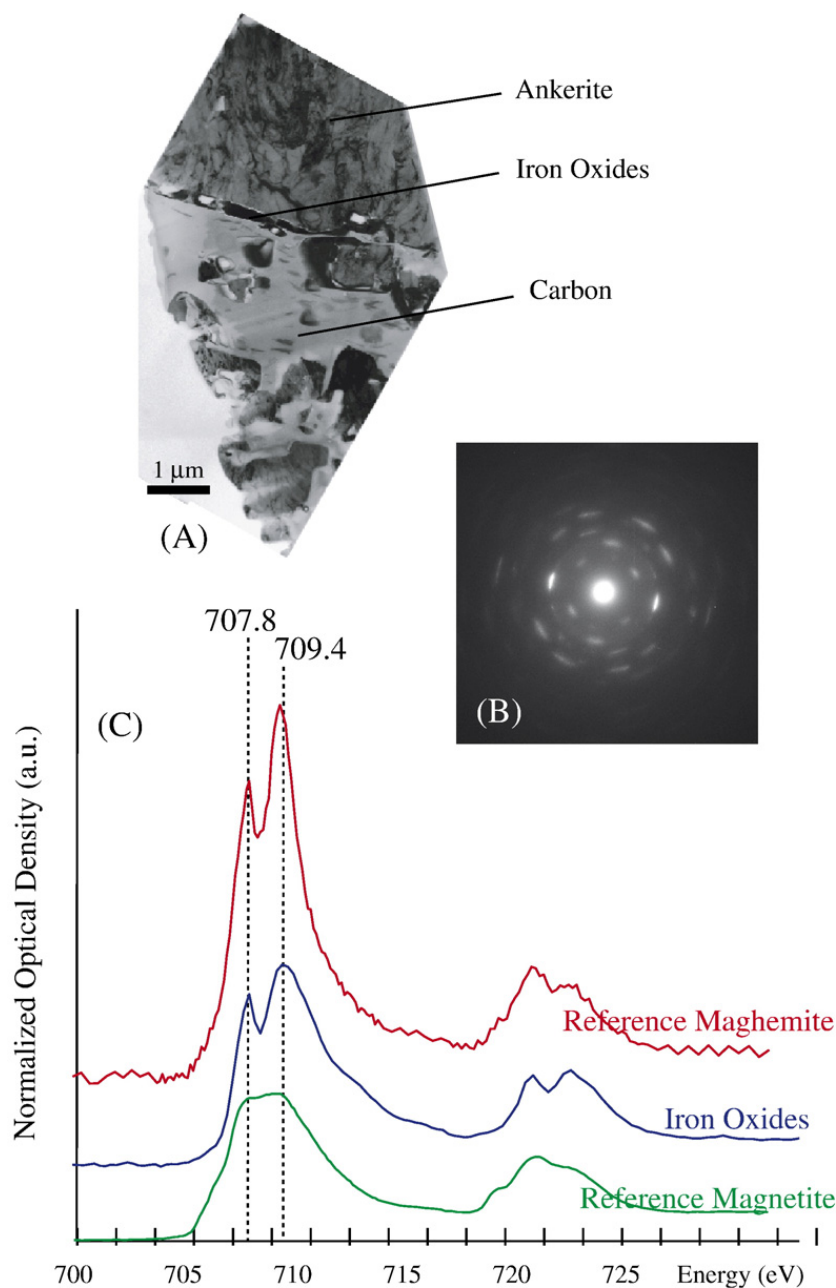
Fig. 9. TEM and STXM study of the layer of iron oxide nanocrystals within a megaspore wall (FIB section 1 described in Fig. 4). A. TEM photomicrograph of the transition between the ankerite corona and the spore wall. B. Electron diffraction pattern of the iron oxide layer. Measured distances (*i.e.* 3.8, 2.8, 2.6, 2.3, and 1.9 Å) are compatible with lattice spacings of magnetite or maghemite (corresponding, respectively, to (102), (212), (031), (203), and (133) lattice planes of magnetite or maghemite). C. NEXAFS spectra at the Fe $L_{2,3}$-edges of iron oxide nanocrystals and reference spectra of maghemite and magnetite. Comparison with reference spectra of maghemite and magnetite suggests that the iron oxide nanocrystals in the spore wall are magnetite with some partial maghemitization.

the other. Testing such a scenario deserves additional investigation, for instance experiments under controlled redox conditions. (3) A third possible scenario is that the different mineralogical layers represent an original biochemical layering; the magnetite layer would represent the transition between the former endospore and the exospore of the cell wall, while the ankerite layer would result from the degradation of the endospore. While we

favour this third scenario, in which all the observed heterogeneities are remnants of primary biochemical heterogeneities (see details below), some future work should be conducted to further test these alternative hypotheses. First, measurements of $^{13}C/^{12}C$ isotope ratios in the 5 μm-thick ankerite layer might document whether ankerite has a ^{13}C-depleted isotopic signature consistent with an organic carbon source or not. Second,

fossilization experiments in the laboratory of modern spores reproducing our experiments under biotic or abiotic conditions may support one of those hypotheses. Finally, other plant tissues, which likely have different original biochemistries, have been described within the Vanoise septaria (Goffé and Villey, 1984). Their characterization using the same set of techniques might provide additional constraints on the origin of the mineralogical heterogeneities we observe.

5.3. Origin of the OM-rich layer

As inferred from modern and fossils analogues, the external layer of megaspore cell walls is mostly composed of sporopollenin. As shown by Nuclear Magnetic Resonance and STXM investigations (Cody et al., 1996; Hemsley et al., 1996), non-metamorphosed sporopollenin contains fatty acids, a variable concentration of alkylphenols and alcohols, and a substantial amount of aromatic and aliphatic polymers. Moreover, it has been shown that sporinite, which originates from the maturation of spores and pollens, can contain a diversity of preserved carbon functional groups (Cody et al., 1996). NEXAFS spectra of non-graphitic OM in the Vanoise spores were found to be similar to those from sporinite in coal (Cody et al., 1996) (Fig. 4) and to display a chemistry compatible with sporopollenin (see Section 4.1). The aliphatic functional groups appear to have been selec-

tively lost (alcohols, *e.g.*, are not detected), whereas the aromatic groups are enhanced. We may thus interpret OM in the megaspore wall as a remnant of the exospore for the following reasons: (1) the exospore is usually the only carbonaceous structure preserved in fossil spores (Hemsley et al., 1996), (2) the OM-rich layer in the Vanoise spore wall shows ornamentations that are highly reminiscent of exospores (Fig. 2), and (Fig. 3) this carbon-rich layer displays organic chemistry consistent with metamorphosed sporopollenin.

5.4. Heterogeneities in the metamorphosed megaspores as fossils of the original biostructure

In this section, we interpret our observations on fossilized spores in the light of the structure of a modern megaspore wall (see Section 2.2). The following discussion is summarized in Fig. 10, which compares the structure of modern megaspore walls as inferred from the literature (*e.g.*, Gabarayeva and Hemsley, 2006) with our observations in the Vanoise fossilized spore wall.

As explained above (see Section 5.3), the non-graphitic carbon in the OM-rich layer within the megaspore walls might be preserved, although metamorphosed, sporopollenin. In contrast, the partially graphitized OM which is observed in the inner area of the exospore (graphitic carbon) may correspond to OM which was originally chemically different. Chemical and textural
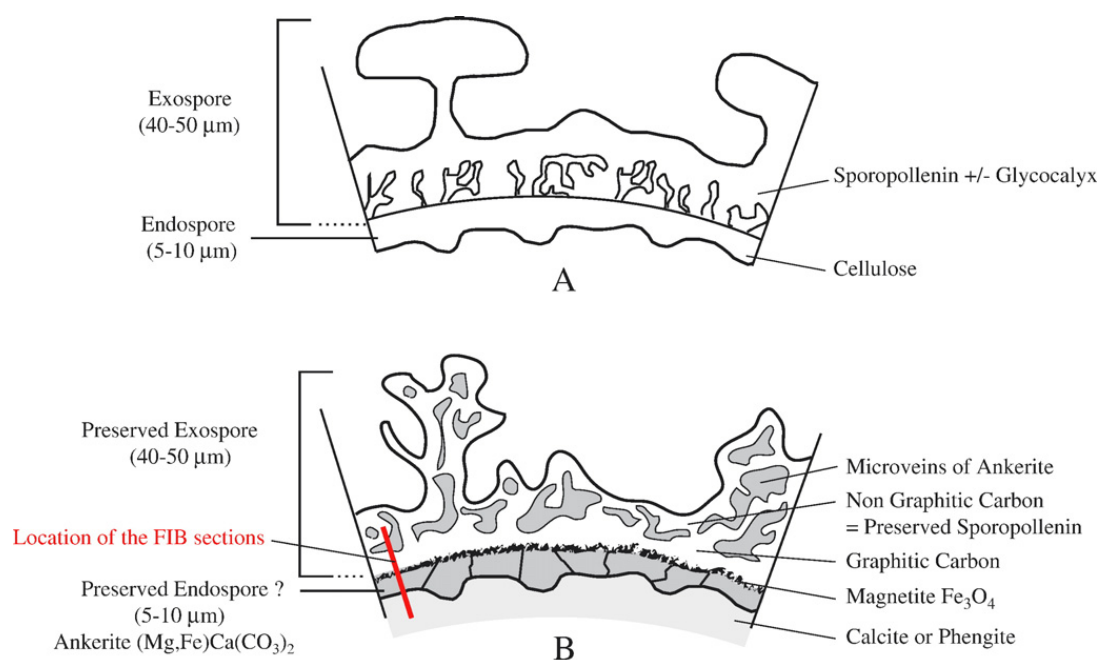

Fig. 10. Schematic comparison between the structure of a modern megaspore wall (A, from Gabarayeva and Hemsley, 2006) and a metamorphosed megaspore wall from Vanoise (B).

heterogeneities have been observed in modern exospores, such as the presence of glycocalyx (glycoprotein), which facilitates the first deposition of sporopollenin during the development of the spore wall structure (see Lugardon, 1995; Gabarayeva and Hemsley, 2006 and reference therein). Hence, the nanoscale heterogeneities observed within the OM-rich layer of the Vanoise megaspore wall may result from the fossilization of the primary biochemical heterogeneities of the exospore (Fig. 10). Such heterogeneities might be preserved as long as the different carbonaceous compounds are not completely transformed into pure, well-crystallized graphite.

Similarly, the mineralogical zonation could result from the mineralization of primary biochemical heterogeneities. The magnetite layer observed within the spore wall of the Vanoise fossils could have precipitated at the transition between the exospore and the former endospore (Fig. 10). This is suggested by the experimental observation of a preferential precipitation of Fe-containing particles at the endospore/exospore transition by Pulido et al. (2005) who incubated microspores in an iron-saturated solution.

The location of the magnetite layer between the inner surface of the OM-rich layer and the ankerite corona, when compared to microspores observed by Pulido et al. (2005), suggests a biogenic origin for the ankerite. Moreover, the ankerite layer displays a non-continuous wavy shape and a maximum thickness of 5 µm, which is of similar magnitude to that observed for endospores in modern spores (Pulido et al., 2005; Gabarayeva and Hemsley, 2006). As stated above, the endospore is mostly composed of cellulose, not chemically resistant and usually not preserved in diagenetic fossil megaspores (Hemsley et al., 1996; Hanel et al., 1999). We thus propose that the ankerite corona observed within the spore wall in association with some OM corresponds to the diagenetic degradation of the cellulose composing the former endospore (Fig. 10). This hypothesis is also supported by previous studies which report the formation of ankerite by selective replacement of OM at an early stage at 2–3 km burial depth and a temperature below 150 °C, during the diagenetic fossilization of biological tissues (Zodrow and Cleal, 1999; Hendry et al., 2000). Moreover, such early diagenetic cementation processes have been demonstrated to be essential in the preservation of non-mineralized organisms (Scott and Hemsley, 1993; Briggs, 2003; Gaines et al., 2005; Zhu et al., 2005). Replacement of the poorly resistant cellulose comprising the endospore by ankerite during early diagenesis would thus explain the preferential location of ankerite beneath the preserved megaspore wall, and more generally the systematic association of ankerite with OM within the septaria.

6. Conclusions and perspectives

In spite of aliphatic carbon losses, some carbonaceous structures such as the external wall of the spores were structurally preserved during high-grade metamorphism and show nanoscale chemical heterogeneities that may result from primary chemical heterogeneities existing within the original biological object. Those chemical heterogeneities were consistently observed by Raman microspectroscopy, TEM, and STXM. These observations are at variance with the common belief that high-grade metamorphism erases all chemical differences in OM. In summary, even after experiencing high-grade metamorphism, chemical, textural, and mineralogical fingerprints of biological structures can be preserved in some rocks; however, the combination of spectroscopic and microscopic methods used in this study is necessary for detecting such features down to the nanometer-scale.

The exceptional preservation of such morphological features provides an opportunity for several additional lines of investigation. First, their non-ambiguous identification, coupled with the possibility of determining their absolute age, might provide unique paleo-environmental information on their sedimentary protoliths. Such original stratigraphic data are normally not obtainable for such metamorphic rocks but were retrieved from exceptional fossils in high-grade metamorphic gneisses from the Variscan Belt, Germany (Hanel et al., 1999). Second, these samples offer new insights on preservation of traces of life despite metamorphism and tectonic exhumation. These megaspores do not exhibit any tectonic deformation as they may have been protected within the carbonated septaria. Such septaria might then allow an exceptional preservation of biological traces and their study may shed new light on biological history over the geological ages. However, a more systematic study on septaria from diverse geological settings and that have undergone various metamorphic conditions will be necessary to better understand this protective role. Moreover, the possibility that an iron oxide/ankerite ring provided a protective barrier to chemical degradation since late diagenesis may also explain their exceptional morphological preservation; this hypothesis also deserves further testing.

Finally, the multi-scale characterization methodology described in this study, which allowed recognition of two distinct types of organic material on the single-cell scale in metamorphic rocks, opens new avenues for studies of fossilized materials in metamorphic or diagenetic rocks and reconstructions of their biological sources. Such recognition is of particular interest in the

study of soft-bodied fossils such as those observed, for example, in Burgess Shale-type fossil deposits (Butterfield, 1995; Orr et al., 1998; Butterfield et al., 2007). In addition, studying intermediate metamorphic stages will also be important in the future to better understand the respective roles of diagenesis and metamorphism on the transformation of soft-bodied fossils (Butterfield et al., 2007).

References

Ahuja, R., Bruhwiler, P.A., Wills, J.M., Johansson, B., Martensson, N., Eriksson, O., 1996. Theoretical and experimental study of the graphite 1s X-ray absorption edges. Phys. Rev., B 54, 14396–14404.

Atamny, F., Blöcker, J., Henschke, B., Schlögl, R., Schedel-Niedrig, T., Keil, M., Bradshaw, A.M., 1992. The reaction of oxygen with graphite: X-ray absorption spectroscopy of carbonaceous materials. J. Phys. Chem. 96, 4522.

Benzerara, K., Yoon, T.-H., Tyliszczak, T., Constantz, B., Spormann, A.M., Brown Jr., G.E., 2004. Scanning transmission X-ray microscopy study of microbial calcification. Geobiology 2, 249–259.

Benzerara, K., Menguy, N., Guyot, F., Vanni, C., Gillet, P., 2005a. TEM study of a silicate carbonate-microbe interface prepared by focused ion beam milling. Geochim. Cosmochim. Acta 69, 1413–1422.

Benzerara, K., Yoon, T.-H., Menguy, N., Tyliszczak, T., Brown Jr., G.E., 2005b. Nanoscale environments associated with bioweathering of a meteoritic Mg–Fe–pyroxene. Proc. Natl. Acad. Sci. U. S. A. 102, 979–982.

Benzerara, K., Menguy, N., López-García, P., Yoon, T.H., Kazmierczak, J., Tyliszczak, T., Guyot, F., Brown Jr., G.E., 2006a. Nanoscale detection of organic signatures in carbonate microbialites. Proc. Natl. Acad. Sci. U. S. A. 103, 9440–9445.

Benzerara, K., Chapon, V., Moreira, D., López-García, P., Heulin, T., Guyot, F., 2006b. Microbial diversity on the Tatahouine meteorite. Meteorit. Planet. Sci. 41, 1249–1265.

Beyssac, O., Rouzaud, J.N., Goffe, B., Brunet, F., Chopin, C., 2002a. Graphitization in high-pressure, low-temperature metamorphic gradient: a HRTEM and Raman microspectroscopy study. Contrib. Mineral. Petrol. 143, 19–31.

Beyssac, O., Goffe, B., Chopin, C., Rouzaud, J.N., 2002b. Raman spectra of carbonaceous material in metasediments: a new geothermometer. J. Metamorph. Geol. 20, 859–871.

Beyssac, O., Goffe, B., Petitet, J.P., Froigneux, E., Moreau, M., Rouzaud, J.N., 2003. On the characterization of disordered and heterogeneous carbonaceous materials using Raman spectroscopy. Spectrochim. Acta, A 59, 2267–2276.

Bluhm, H., Andersson, K., Araki, T., Benzerara, K., Brown, G.E., Dynes, J.J., Ghosal, S., Gilles, M.K., Hansen, H.-C., Hemminger, J.C., Hitchcock, A.P., Ketteler, G., Kilcoyne, A.L.D., Kneedler, E., Lawrence, J.R., Leppard, G.G., Majzlam, J., Mun, B.S., Myneni, S.C.B., Nilsson, A., Ogasawara, H., Ogletree, D.F., Pecher, K., Salmeron, M., Shuh, D.K., Tonner, B., Tyliszczak, T., Warwick, T., Yoon, T.H., 2006. Soft X-ray microscopy and spectroscopy at the molecular environmental science beamline at the advanced light source. J. Electron Spectrosc. Relat. Phenom. 150, 86–104.

Boyce, C.K., Cody, G.D., Feser, M., Jacobsen, C., Knoll, A.H., Wirick, S., 2002. Organic chemical differentiation within fossil plant cell walls detected with X-ray spectromicroscopy. Geology 30, 1039–1042.

Brasier, M.D., Green, O.R., Jephcoat, A.P., Kleppe, A.K., Van Kranendonk, M.J., Lindsay, J.F., Steele, A., Grassineau, N.V., 2002. Questioning the evidence for earth's oldest fossils. Nature 416, 76–81.

Brice-Profeta, S., Arrio, M.A., Tronc, E., Menguy, N., Letard, I., Moulin, C.C.D., Nogues, M., Chaneac, C., Jolivet, J.P., Sainctavit, P., 2005. Magnetic order in gamma-Fe_2O_3 nanoparticles: a XMCD study. J. Magn. Magn. Mater. 288, 354–365.

Briggs, D.E.G., 2003. The role of decay and mineralization in the preservation of soft-bodied fossils. Annu. Rev. Earth Planet. Sci. 31, 275–301.

Buseck, P.R., Huang, B.J., 1985. Conversion of carbonaceous material to graphite during metamorphism. Geochim. Cosmochim. Acta 49, 2003–2016.

Butterfield, N.J., 1995. Secular distribution of Burgess-Shale-type preservation. Lethaia 28, 1–13.

Butterfield, N.J., 2003. Exceptional fossil preservation and the Cambrian explosion. Integr. Comp. Biology 43, 166–177.

Butterfield, N.J., Balthasar, U., Wilson, L.A., 2007. Fossil diagenesis in the Burgess Shale. Palaeontology 50, 537–543.

Cantrill, D.J., Webb, J.A., 1998. Permineralized pleuromeid lycopsid remains from the early Triassic Arcadia formation, Queensland, Australia. Rev. Palaeobot. Palynol. 102, 189–211.

Cody, G.D., Botto, R.E., Ade, H., Wirick, S., 1996. The application of soft X-ray microscopy to the in-situ analysis of sporinite in coal. Int. J. Coal Geol. 32, 69–86.

Cody, G.D., Ade, H., Wirick, S., Mitchell, G.D., Davis, A., 1998. Determination of chemical-structural changes in vitrinite

accompanying luminescence alteration using C-NEXAFS analysis. Org. Geochem. 28, 441–455.

Cope, J.C.W., Curtis, C.D., 2000. Palaeobiology meets geochemistry: concretions as tombs. J. Geol. Soc. 157, 163–164.

Cottnam, C.F., Hemsley, A.R., Rossler, R., Collinson, M.E., Brain, A.P.R., 2000. Diversity of exine structure in Upper Carboniferous (Westphalian) Selaginellalean megaspores. Rev. Palaeobot. Palynol. 109, 33–44 (plate I, figure 1).

Derenne, S., Largeau, C., 2001. A review of some important families of refractory macromolecules: composition, origin, and fate in soils and sediments. Soil Sci. 166, 833–847.

Dutkiewicz, A., Volk, H., George, S.C., Ridley, J., Buick, R., 2006. Biomarkers from Huronian oil-bearing fluid inclusions: an uncontaminated record of life before the Great Oxidation Event. Geology 34, 437–440.

Dynes, J.J., Tyliszczak, T., Araki, T., Lawrence, J.R., Swerhone, G.D.W., Leppard, G.G., Hitchcock, A.P., 2006. Speciation and quantitative mapping of metal species in microbial biofilms using scanning transmission X-ray microscopy. Environ. Sci. Technol. 40, 1556–1565.

Ellenberger, F., 1958. Etude géologique du pays de Vanoise. Explication de la carte géologique de la France. 561 pp.

Erdtman, G., 1969. Handbook of Palynology — An Introduction to the Study of Polllen Grains and Spores. Munksgaard, Copenhagen.

Franz, G., Mosbrugger, V., Menge, R., 1991. Carbo-Permian pteridophyll leaf fragments from an amphibolite facies basement, Tauern Window, Austria. Terra Nova 3, 137–141.

Gabarayeva, N.I., Hemsley, A.R., 2006. Merging concepts: the role of self-assembly in the development of pollen wall structure. Rev. Palaeobot. Palynol. 138, 121–139.

Gaines, R.R., Kennedy, M.J., Droser, M.L., 2005. A new hypothesis for organic preservation of Burgess Shale taxa in the middle Cambrian Wheeler Formation, House Range, Utah. Palaeogeogr. Palaeoclimatol. Palaeoecol. 220, 193–205.

Gillet, P., Goffe, B., 1988. On the significance of aragonite occurrences in the western Alps. Contrib. Mineral. Petrol. 99, 70–81.

Goffé, B., Villey, M., 1984. Texture d'un matériel carboné impliqué dans un métamorphisme haute pression-basse température (Alpes françaises). Les hautes pressions influencent-elles la carbonification? Bull. Minéral. 107, 81–93.

Grauvogel-Stamm, L., Duringer, P., 1983. Annalepsis Zeilleri Fliche 1910 Emend., un organe reproducteur de Lycophyte de la Lettenkohle de l'Est de la France. Morphologie, spores in situ et paléoécologie. Geol. Rundsch. 72, 23–51.

Grauvogel-Stamm, L., Lugardon, B., 2001. The Triassic Lycopsids Pleuromeia and Annalepis: relationships, evolution and origin. Am. Fern J. 91, 115–149.

Grauvogel-Stamm, L., Lugardon, B., 2004. The spores of the Triassic Lycopsid Pleuromeia Sternbergii (Munster) Corda: morphology, ultrastructure, phylogenetic implications, and chronostratigraphic inferences. Int. J. Plant Sci. 165, 631–650.

Hanel, M., Montenari, M., Kalt, A., 1999. Determining sedimentation ages of high-grade metamorphic gneisses by their palynological record: a case study in the Northern Schwarzwald (Variscan Belt, Germany). Int. J. Earth Sci. 88, 49–59.

Heaney, P.J., Vicenzi, E.P., Giannuzzi, L.A., Livi, K.T.J., 2001. Focused ion beam milling: a method of site-specific sample extraction for microanalysis of Earth and planetary materials. Am. Mineral. 86, 1094–1099.

Hemsley, A.R., Scott, A.C., Barrie, P.J., Chaloner, W.G., 1996. Studies of fossil and modern spore wall biomacromolecules using C-13 solid state NMR. Ann. Bot. 78, 83–94.

Hendry, J.P., Wilkinson, M., Fallick, A.E., Haszeldine, R.S., 2000. Ankerite cementation in deeply buried Jurassic sandstone reservoirs of the central North Sea. J. Sediment. Res. 70, 227–239.

Hitchcock, A.P., 2000. AXis2000 software (ver2.1n), http://unicorn.mcmaster.ca/aXis2000.html.

Hitchcock, A.P., 2001. Chemical mapping with soft X-ray spectromicroscopy. Am. Lab. 33, 30–36.

Jacobsen, C., Wirick, S., Flynn, G., Zimba, C., 2000. Soft X-ray spectroscopy from image sequences with sub-100 nm spatial resolution. J. Microsc. (Oxford) 197, 173–184.

Jokic, A., Cutler, J.N., Ponomarenko, E., van der Kamp, G., Anderson, D.W., 2003. Organic carbon and sulphur compounds in wetland soils: insights on structure and transformation processes using K-edge XANES and NMR spectroscopy. Geochim. Cosmochim. Acta 67, 2585–2597.

Jull, A.J.T., Courtney, C., Jeffrey, D.A., Beck, J.W., 1998. Isotopic evidence for a terrestrial source of organic compounds found in the Martian meteorites ALH 84001 and EETA 79001. Science 279, 365–369.

Kempe, A., Wirth, R., Altermann, W., Stark, R.W., Schopf, J.W., Heckl, W.M., 2005. Focussed ion beam preparation and *in situ* nanoscopic study of Precambrian acritarchs. Precambrian Res. 140, 36–54.

Kinyangi, J., Solomon, D., Liang, B.I., Lerotic, M., Wirick, S., Lehmann, J., 2006. Nanoscale biogeocomplexity of the organomineral assemblage in soil: application of STXM microscopy and C 1s-NEXAFS spectroscopy. Soil Sci. Soc. Am. J. 70, 1708–1718.

Knoll, A.H., Walter, M.R., 1992. Latest Proterozoic stratigraphy and Earth history. Nature 356, 673–678.

Kretz, R., 1983. Symbols for rock-forming minerals. Am. Mineral. 68, 277–279.

Lugardon, B., 1995. Exine formation in Chamaecyparis Lawsoniana (Cupressaceae) and a discussion on Pteridophyte exospore and Gymnosperm exine ontogeny. Rev. Palaeobot. Palynol. 85, 35–51.

Lugardon, B., Grauvogel-Stamm, L., Dobruskina, I., 2000. Comparative ultrastructure of the megaspores of the Triassic Lycopsid Pleuromeia Rossica Neuburg. C. R. Acad. Sci., Sér. 330 I, 501–508.

Macluf, C.C., Morbelli, M.A., Giudice, G.E., 2003. Morphology and ultrastructure of megaspores and microspores of Isoetes Savatieri Franchet (Lycophyta). Rev. Palaeobot. Palynol. 126, 197–209 (plate V).

Massonne, H.J., Szpurka, Z., 1997. Thermodynamic properties of white micas on the basis of high-pressure experiments in the systems K_2O–MgO–Al_2O_3–SiO_2–H_2O and K_2O–$FeOAl_2O_3$–SiO_2–H_2O. Lithos 41, 229–250.

Morbelli, M.A., 1995. Megaspore wall in Lycophyta, ultrastructure and function. Rev. Palaeobot. Palynol. 85, 1–12.

Moorbath, S., 2005. Palaeobiology — dating earliest life. Nature 434, 155.

Myneni, S.C.B., 2002. Soft X-ray spectroscopy and spectromicroscopy studies of organic molecules in the environment. Rev. Mineral. Geochem. 49, 485–579.

Orr, P.J., Briggs, D.E.G., Kearns, S.L., 1998. Cambrian Burgess Shale animals replicated in clay minerals. Science 281, 1173–1175.

Peng, G., Van Elp, J., Jang, H., Que, L., Armstrong, W.H., Cramer, S.P., 1995. L-edge X-ray absorption and X-ray magnetic circular dichroism of oxygen-bridged dinuclear iron complexes. J. Am. Chem. Soc. 117, 2515–2519.

Powell, W., 2003. Greenschist-Facies Metamorphism of the Burgess Shale and its implications for models of fossil formation and preservation. Can. J. Earth Sci. 40, 13–25.

Pulido, A., Bakos, F., Castillo, A., Vallés, M.P., Barnabas, B., Olmedilla, A., 2005. Cytological and ultrastructural changes induced in anther

and isolated-micro spore cultures in barley: Fe deposits in isolated-micro spore cultures. J. Struct. Biol. 149, 170–181.

Schopf, J.W., Kudryavtsev, A.B., Agresti, D.G., Wdowiak, T.J., Czaja, A.D., 2002. Laser Raman imagery of earth's earliest fossils. Nature 416, 73–76.

Schumacher, M., Christl, I., Scheinost, A.C., Jacobsen, C., Kretzschmar, R., 2005. Chemical heterogeneity of organic soil colloids investigated by scanning transmission X-ray microscopy and C-1s NEXAFS microspectroscopy. Environ. Sci. Technol. 39, 9094–9100.

Scott, A.C., Hemsley, A.R., 1993. Controls upon the ultrastructural preservation of sporinite. Fuel 72, 1145–1149.

Stohr, J., 1992. NEXAFS Spectroscopy; Springer Series in Surface Science. Springer-Verlag, Berlin, p. 25.

Van Zuilen, M.A., Lepland, A., Teranes, J., Finarelli, J., Wahlen, M., Arrhenius, G., 2003. Graphite and carbonates in the 3.8 Ga old Isua Supracrustal Belt, Southern West Greenland. Precambrian Res. 126, 331–348.

Wang, Z.Q., Wang, L.X., 1982. A new species of the Lycopsid Pleuromeia from the early Triassic of Shanxi, China, and its ecology. Palaeontology 25, 215–225.

Wopenka, B., Pasteris, J.D., 1993. Structural characterization of kerogens to granulite–facies graphite — applicability of Raman microprobe spectroscopy. Am. Mineral. 78, 533–557.

Yoon, T.H., Johnson, S.B., Benzerara, K., Doyle, C.S., Tyliszczak, T., Shuh, D.K., Brown Jr., G.E., 2004. In situ characterization of aluminum-containing mineral-microorganism aqueous suspensions using scanning transmission X-ray microscopy. Langmuir 20, 10361–10366.

Zhu, M., Babcock, L.E., Steiner, M., 2005. Fossilization modes in the Chengjiang Lagerstatte (Cambrian of China): testing the roles of organic preservation and diagenetic alteration in exceptional preservation. Palaeogeogr. Palaeoclimatol. Palaeoecol. 220, 31–46.

Zodrow, E.L., Cleal, C.J., 1999. Anatomically preserved plants in siderite concretions in the shale split of the Foord Seam; mineralogy, geochemistry, genesis (Upper Carboniferous, Canada). Int. J. Coal Geol. 41, 371–393.